Low Rank Magnetic Resonance Fingerprinting

Gal Mazor[1], Lior Weizman[1], Assaf Tal[2], and Yonina C. Eldar[1]

[1]*Department of EE, Technion, Haifa, Israel*
[2]*Department of Chemical Physics, Weizmann Institute of Science, Rehovot, Israel*

***Abstract*—Magnetic Resonance Fingerprinting (MRF) is a relatively new approach that provides quantitative MRI using randomized acquisition. Extraction of physical quantitative tissue values is preformed off-line, based on acquisition with varying parameters and a dictionary generated according to the Bloch equations. MRF uses hundreds of radio frequency (RF) excitation pulses for acquisition, and therefore high under-sampling ratio in the sampling domain (k-space) is required. This under-sampling causes spatial artifacts that hamper the ability to accurately estimate the quantitative tissue values. In this work, we introduce a new approach for quantitative MRI using MRF, called Low Rank MRF. We exploit the low rank property of the temporal domain, on top of the well-known sparsity of the MRF signal in the generated dictionary domain. We present an iterative scheme that consists of a gradient step followed by a low rank projection using the singular value decomposition. Experiments on real MRI data demonstrate superior results compared to conventional implementation of compressed sensing for MRF at 15% sampling ratio.**

I. Introduction

Magnetic resonance fingerprinting (MRF) [1] is a relatively new concept in quantitative Magnetic Resonance Imaging (MRI). In contrast to traditional MRI, where repeated, serial acquisition of data is carried out, MRF uses pseudo-randomized acquisitions to generate many different imaging contrasts, acquired at a high under-sampling ratio. MRF causes the signals from different materials or tissues to have a unique reaction, a "fingerprint", that is simultaneously a function of the multiple material properties under investigation. By matching this unique reaction to a set of expected simulated patterns, quantitative parameters can be extracted, and from them traditional MRI images may be produced off-line. This approach saves valuable scan time, and has proven to be extremely efficient [1].

In MRF, a random pulse pattern is executed during the scan, and each tissue responds to this sequence in a different manner. By varying the acquisition parameters (e.g. repetition time (TR), echo time (TE), radio frequency (RF) flip angle and the readout trajectory), unique signals are generated from different tissue types. After acquisition, a pattern recognition algorithm is used to match the acquired signal to an entry from a dictionary of possible tissue candidates. The dictionary entries are created by simulating the acquisition sequence on a range of parameters, demonstrating different biological tissues. The simulations are based on the Bloch equations and use the T1 and T2 time constants of the tissues, together with the selected random pulse pattern. The resulting dictionary demonstrates the reaction of the different materials to the pulse sequence. The quantitative parameters, such as the tissue's T1 and T2 relaxation times, can be simultaneously retrieved from the data by matching the signature acquired to the most correlated entry in the dictionary.

In MRI, data is acquired in the spatial image domain (k-space), where the acquisition time of a high resolution, 3D MRI lasts a few minutes. Since MRF is based on rapid acquisition of multiple contrasts, severe under-sampling is needed to obtain the temporal resolution required for MRF. In the original MRF paper, reconstruction from under-sampled k-space data is preformed by zero-filling of the missing k-space values [1]. Later works added sparse representation and compressed sensing (CS) methods [2] to improve reconstruction. Davies et al. [3] developed an approach called BLIP (BLoch response recovery via Iterative Projection) that is based on gradient descent and projection onto the dictionary sub-space. Zhe Wang et al. [4] suggested a method that exploits the sparsity in the wavelet domain of each imaging contrast, together with changing the acquisition trajectories between time stamps. Although those techniques have shown improved performance over the original MRF approach, they do not exploit the temporal similarity across frames, which is a fundamental nature of the MRF acquisition scheme. Such similarity is exploited, via modeling the data as low-rank data, in many MRI applications with high temporal resolution, such as cardiac imaging [5] and functional MRI [6].

An initial work describing the implementation of low-rank model for MRF has been developed recently [7]. Here, we apply different a reconstruction algorithm and compare our low-rank based MRF reconstruction to other CS approaches. We exploit the low-rank property of the temporal domain of MRF, via an iterative scheme that consists of a gradient step followed by a low rank projection using the singular value decomposition. The low rank estimate is then fit to one of the dictionary elements in an iterative fashion, in order to identify the tissue. Experimental results are presented using MRI data of a human patient, and demonstrate superior performance using only 15% of k-space data.

II. Method

A. Problem formulation

MRF data consists of multiple frames, acquired in the image's conjugate Fourier domain (a.k.a k-space) of the image, where each frame is acquired with different acquisition parameters. We stack the measurements into a $Q \times L$ matrix $\mathbf{Y}$, where L is the number of frames and Q is the number

This work was supported by the Ministry of Science, by the ISF I-CORE joint research center of the Technion and the Weizmann Institute, Israel and by the European Union's Horizon 2020 research and innovation programme under grant agreement No. 646804-ERC-COG-BNYQ.

978-1-4577-0220-4/16/$31.00 ©2016 IEEE

of k-space samples in each frame. Every column in $\mathbf{Y}$ is an under-sampled Fourier transform of image frame, $\mathbf{X}_{:,\mathbf{i}}$:

$$\mathbf{Y} = [F_u\{\mathbf{X}_{:,1}\}, ..., F_u\{\mathbf{X}_{:,L}\}] \tag{1}$$

where $F_u\{\cdot\}$ denotes an under-sampled Fourier transform. A row $\mathbf{X}_{j,:}$ represents a tissue characterized by its relaxation times of the tissue, T1 and T2, and its proton density, PD, grouped as a row vector:

$$\mathbf{\Theta}_2^j = [T1^j, T2^j, PD^j], 1 \leq j \leq N \tag{2}$$

Each column, $\mathbf{X}_{:,i}$ is acquired using different parameters, stacked as a column vector:

$$\mathbf{\Theta}_1^i = [TR^i, TE^i, RF^i]^T, 1 \leq i \leq L \tag{3}$$

where TR and TE are the repetition time and time to echo and RF represents the flip angle of the RF pulse. Therefore, $\mathbf{X}_{j,:} = f(\mathbf{\Theta}_1, \mathbf{\Theta}_2^j)$ where $f\{\cdot\}$ represents the operation of the Bloch equations. Note that we omit the off resonance parameter (which appeared in the original MRF paper [1]), since our sequence is based on the fast imaging with steady state precession (FISP) sequence, which has been proven to be insensitive to off resonance effects [8].

The goal in MRF is to recover, from the measurements $\mathbf{Y}$, the imaging contrasts $\mathbf{X}$ and the underlying quantitative parameters of each pixel defined in (2), under the assumption that every pixel in the image contains a single type of tissue and that $\mathbf{\Theta}_1$ is known.

Recovery is performed by defining a dictionary that consists of simulating the signal generated from M tissues using Bloch equations (represented as M different combinations of T1 and T2 relaxation times), when the L-length acquisition sequence defined in (3) is used. As a result, we obtain a dictionary $\mathbf{D}$ of dimensions $M \times L$. The proton density (PD) is not simulated in the dictionary, as it is the gain used to match the Bloch simulation performed on a single spin to the signal obtained from a pixel containing multiple spin. It can be easily determined when the T1 and T2 maps are known. After successful recovery of $\mathbf{X}$, each row in $\mathbf{X}$ is matched to a single row in the dictionary, and in that way the underlying parameters T1, T2 are determined.

B. Previous Methods

The approach suggested in the original MRF paper [1] matches dictionary items to the acquired data using matched filtering:

$$\begin{aligned}
&\widehat{\mathbf{X}}_{:,i} = F^H\{\mathbf{Y}_{:,i}\}\ \forall i \\
&\widehat{PD}^j = \max\left\{\max_{k_j}\left\{\frac{\text{Re}\{<\mathbf{D}_{k_j}, \widehat{\mathbf{X}}_{j,:}>\}}{\left\|\mathbf{D}_{k_j}\right\|_2}\right\}, 0\right\}\ \forall j \\
&\hat{T}_1^j, \hat{T}_2^j = \text{LUT}(k_j)
\end{aligned} \tag{4}$$

where $F^H\{\cdot\}$ is a zero-filling inverse Fourier transform, k_j are the matching dictionary indices, j is a spatial index and i is the temporal index, representing the i-th frame in the acquisition. The parameter maps are extracted from a look up table (LUT), holding the values of T1 and T2 for each k_j.

Davies et al. [3] suggested a method incorporating sparsity of the data in the dictionary domain (i.e., each pixel is represented by at most one dictionary item), referred to as the BLoch response recovery via Iterative Projection (BLIP) algorithm. BLIP consists of iterating between two main steps: A gradient step that enforces consistency with the measurements, and a projection step that matches each row of $\mathbf{X}$ to a single dictionary item, as described in (4). Wang et al. [4] added an additional constraint that enforces sparsity in the wavelet domain of each imaging frame, $\mathbf{X}_{:,i}$.

C. Low Rank MRF

Low Rank MRF generalizes BLIP by exploiting temporal similarity across time points (columns of $\mathbf{X}$), which is a fundamental nature of MRF. This similarity exists since the same object is acquired, using similar acquisition parameters, in each frame. Typical values for the dimensions of L and N are $L = 200$ and $N = 4096$ (200 excitations for the acquisition of 64x64 images). Experimentally, the rank of $\mathbf{X}$ in such acquisition scenarios is lower than 15. This low-rank property of $\mathbf{X}$ can be exploited for improved reconstruction using the following optimization problem:

$$\begin{aligned}
\underset{\mathbf{X}_{:,i}}{\text{minimize}} \quad & \sum_i \|\mathbf{Y}_{:,i} - F_u\{\mathbf{X}_{:,i}\}\|_2^2 \\
\text{subject to} \quad & \text{rank}(\mathbf{X}) \leq k \\
& \mathbf{X} = \mathbf{RD}
\end{aligned} \tag{5}$$

where k is the rank of the matrix, defined as a fixed pre-chosen parameter, and $\mathbf{R}$ is a matrix with one sparse rows that contains the corresponding PD value for each row of $\mathbf{X}$. We approximate the solution of (5) by using gradient projection, where the low-rank projection is performed in every iteration while the sparsity constraint is enforced only every $m \geq 1$ steps. Our algorithms, referred to as magnetic resonance Fingerprint with LOw Rank (FLOR), is described in Algorithm 1, where the parameters μ, k and m are chosen experimentally. By setting $m = 1$ in Algorithm 1 and removing the SVD step, FLOR reduces to BLIP [3].

Algorithm 1 FLOR - MRF with LOw Rank

Given a set of under-sampled k-space images: $\mathbf{Y}$
Initialization: $\mu, k, m, \mathbf{X}^0 = \mathbf{0}$
Iterate until convergence:

- Iterate over m iterations:
  - Gradient step:
    $\widehat{\mathbf{Z}}_{:,i}^{n+1} = \widehat{\mathbf{X}}_{:,i}^n - \mu F^H\{F_u\{\mathbf{X}_{:,i}\} - \mathbf{Y}_{:,i})\}\ \forall i$
  - Project into low rank sub-space:
    $[\mathbf{U}, \mathbf{S}, \mathbf{V}] = svd(\widehat{\mathbf{Z}}_{:,:}^{n+1})$
    Keep only the k largest singular values $\{\sigma\}_i$ in S
    $\sigma_i = \begin{cases} \sigma_i & i \leq k \\ 0 & otherwise \end{cases}$
    $\widehat{\mathbf{X}}_{:,:}^{n+1} = \mathbf{USV}^H$
- Project into the dictionary sub-space:
  $\widehat{PD}^j = \max\left\{\max_{k_i}\left\{\frac{Re<\mathbf{D}_{k_j}, \widehat{\mathbf{X}}_{j,:}^{n+1}>}{\left\|\mathbf{D}_{k_j}\right\|_2}\right\}, 0\right\} \forall j$
  $\widehat{\mathbf{X}}_{j,:}^{n+1} = \widehat{PD}^j \mathbf{D}_{k_j} \forall j$

Restore maps: $\hat{T}_1^j, \hat{T}_2^j = LUT(k_i), \widehat{PD}^j$

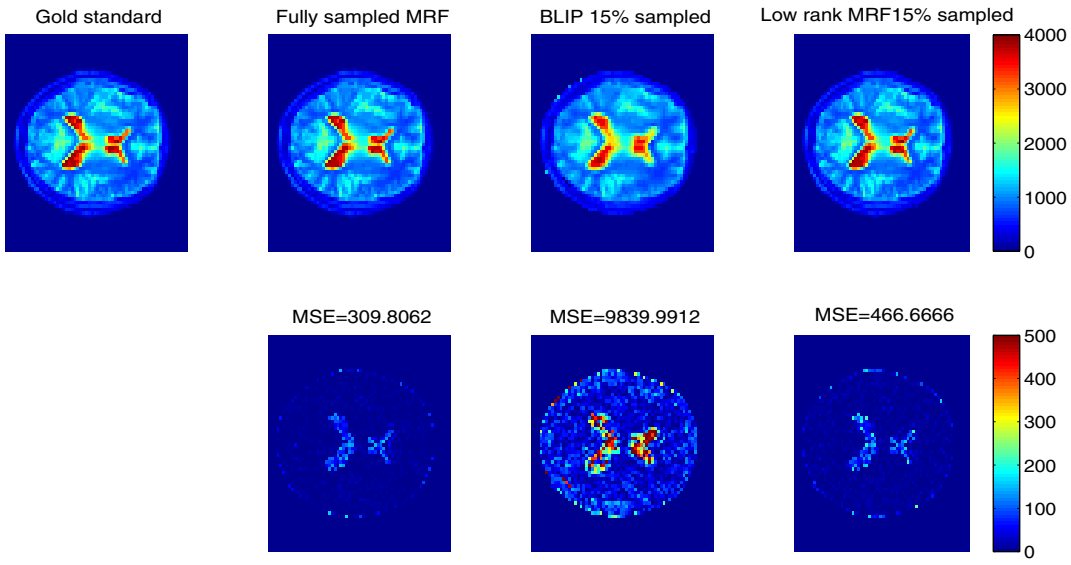

Fig. 1: Results of T1 reconstruction. Top: Gold standard, reconstruction using conventional MRF from 100% of the data, followed by BLIP and low-rank MRF reconstructions from 15% of the data. Bottom: Reconstruction error.

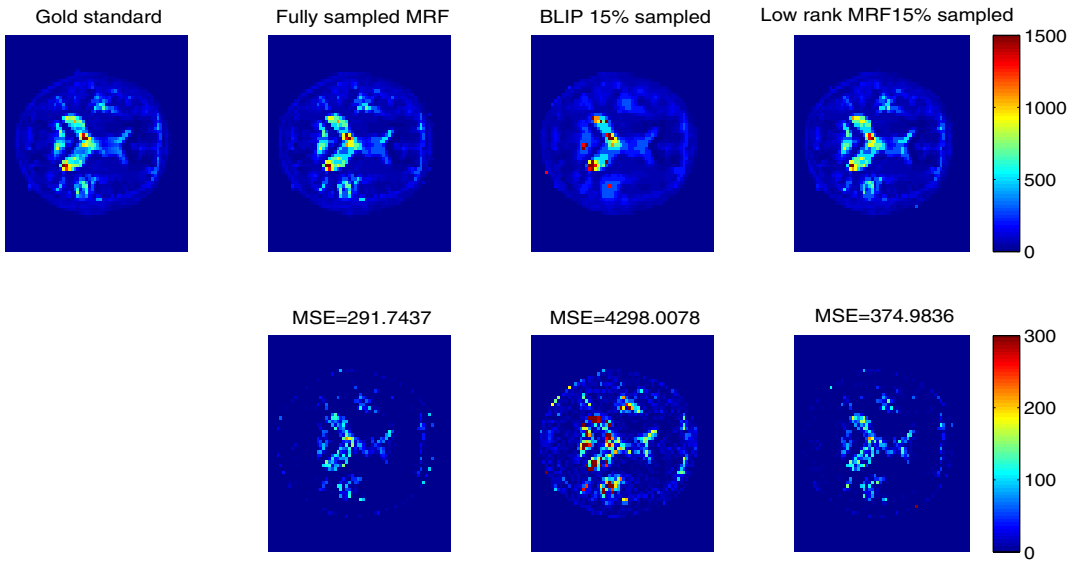

Fig. 2: Results of T2 reconstruction. Top: Gold standard, reconstruction using conventional MRF from 100% of the data, followed by BLIP and low-rank MRF reconstructions from 15% of the data. Bottom: Reconstruction error.

III. Experimental Results

This section describes MRI experiments that were carried using a brain scan of a healthy subject. The experimental procedures involving human subjects described in this paper were approved by the Institutional Review Board of Tel-Aviv Sourasky Medical Center, Israel. We used T1,T2 and PD matrices that were obtained by DESPOT1 and DESPOT2 [9] after improvements as described in [10]. Those maps serve as the gold standard in our experiments. In addition, the FISP pulse sequence was simulated with constant TE of 2ms, random TR values in the range of 0-14ms, and pseudo random flip angles of RF pulses in the range of 0-30 degrees [8]. Complex Gaussian zero-mean noise with $\sigma = 0.5$ was added to the data which was under-sampled to acquire only 15% of the k-space in each TR (randomly, using polynomial distribution of order 4 [11]). Note that the SNR is 110 calculated as the mean value of the absolute gold standard measurements divided by mean value of the absolute noise matrix. Data was fed as an input to BLIP and FLOR. In addition, we performed reconstruction using 100% of the data via conventional MRF, for comparison purposes (results of [4] were very similar to BLIP and are therefore omitted).

We used the same dictionary for all the algorithms, simulating T1 values of [100:20:2000,2300:300:5000] ms and

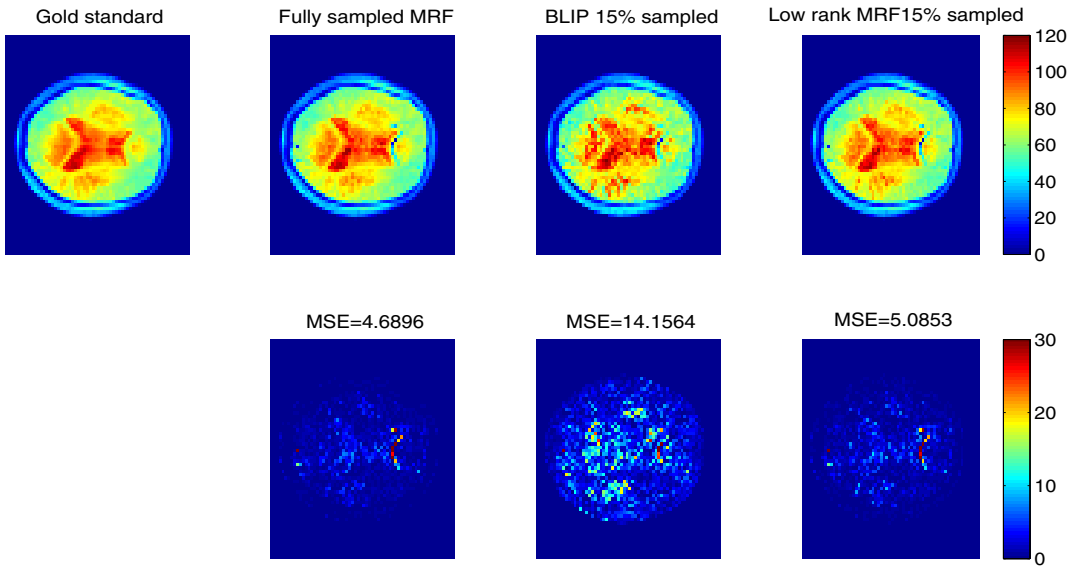

Fig. 3: Results of PD reconstruction. Top: Gold standard, reconstruction using conventional MRF from 100% of the data, followed by BLIP and low-rank MRF reconstructions from 15% of the data. Bottom: Reconstruction error.

T2 values of [20:5:100,110:10:200,300:200:1900] ms. This range covers the relaxation times values that can be found in a healthy brain scan [12]. The tuning parameter and the number of iterations for the internal loop of Algorithm 1 were experimentally set as $\mu = 0.5$ and $m = 30$.

For quantitative error analysis, we calculated the MSE between each quantitative map estimation and the gold standard, defined as: $\frac{1}{N}\sum_j(\theta_i^j - \hat{\theta}_i^j)^2$, where N is the number of pixels in the map and θ_i and $\hat{\theta}_i$ represent a gold standard map (T1,T2 or PD) and its corresponding reconstructed map, respectively, and j is a spatial index.

Figures 1,2 and 3 show the resulting maps for the recovery of T1, T2 and PD maps, respectively. It can be seen that low-rank MRF reconstruction from 15% of data outperforms BLIP, and provides error in the level obtained by MRF using 100% of data. Note that the conventional MRF maps were generated using 100% of the data without noise, and are used for comparison against fully sampled data. The errors in those conventional MRF maps are quantization errors that arise from the discretization in the dictionary only.

IV. Conclusions

We presented the FLOR method for high quality reconstruction of quantitative MRI data using MRF, by exploiting the low-rank property of the MRF scheme. Thanks to the fact that we exploit low-rank on top of the well known sparsity of MRF in the dictionary matching domain, we are able to obtain high quality reconstruction from highly under-sampled data and provide results that are comparable to conventional MRF from 100% of the data, using only 15% of the data. In addition, comparison against CS-based methods for MRF shows the added value of low-rank based reconstruction. Future work will focus on exploiting spiral acquisition trajectories, which were proven to be successful in a few MRF applications, in conjunction with low-rank MRF.

References

[1] D. Ma *et al.*, "Magnetic resonance fingerprinting," *Nature*, vol. 495, no. 7440, pp. 187–192, 2013.

[2] Y. C. Eldar, *Sampling Theory: Beyond Bandlimited Systems*. Cambridge University Press, 2015.

[3] M. Davies, G. Puy, P. Vandergheynst, and Y. Wiaux, "A compressed sensing framework for magnetic resonance fingerprinting," *SIAM Journal on Imaging Sciences*, vol. 7, no. 4, pp. 2623–2656, 2014.

[4] Z. Wang, H. Li, Q. Zhang, J. Yuan, and X. Wang, "Magnetic resonance fingerprinting with compressed sensing and distance metric learning," *Neurocomputing*, vol. 174, pp. 560–570, 2016.

[5] B. Zhao *et al.*, "Low rank matrix recovery for real-time cardiac mri," in *Biomedical Imaging: From Nano to Macro, 2010 IEEE International Symposium on*, pp. 996–999, IEEE, 2010.

[6] M. Chiew, S. M. Smith, P. J. Koopmans, N. N. Graedel, T. Blumensath, and K. L. Miller, "k-t faster: Acceleration of functional mri data acquisition using low rank constraints," *Magnetic resonance in medicine*, vol. 74, no. 2, pp. 353–364, 2015.

[7] B. Zhao, "Model-based iterative reconstruction for magnetic resonance fingerprinting," in *Image Processing (ICIP), 2015 IEEE International Conference on*, pp. 3392–3396, IEEE, 2015.

[8] Y. Jiang *et al.*, "MR fingerprinting using fast imaging with steady state precession (fisp) with spiral readout," *Magnetic resonance in medicine*, vol. 74, no. 6, pp. 1621–1631, 2015.

[9] S. C. Deoni, T. M. Peters, and B. K. Rutt, "High-resolution T1 and T2 mapping of the brain in a clinically acceptable time with despot1 and despot2," *Magnetic resonance in medicine*, vol. 53, pp. 237–241, 2005.

[10] G. Liberman, Y. Louzoun, and D. Ben Bashat, "T1 mapping using variable flip angle spgr data with flip angle correction," *Journal of Magnetic Resonance Imaging*, vol. 40, no. 1, pp. 171–180, 2014.

[11] M. Lustig *et al.*, "Compressed sensing MRI," *Signal Processing Magazine, IEEE*, vol. 25, no. 2, pp. 72–82, 2008.

[12] J. Vymazal *et al.*, "T1 and T2 in the brain of healthy subjects, patients with parkinson disease, and patients with multiple system atrophy: relation to iron content 1," *Radiology*, vol. 211, no. 2, pp. 489–495, 1999.